Highlights

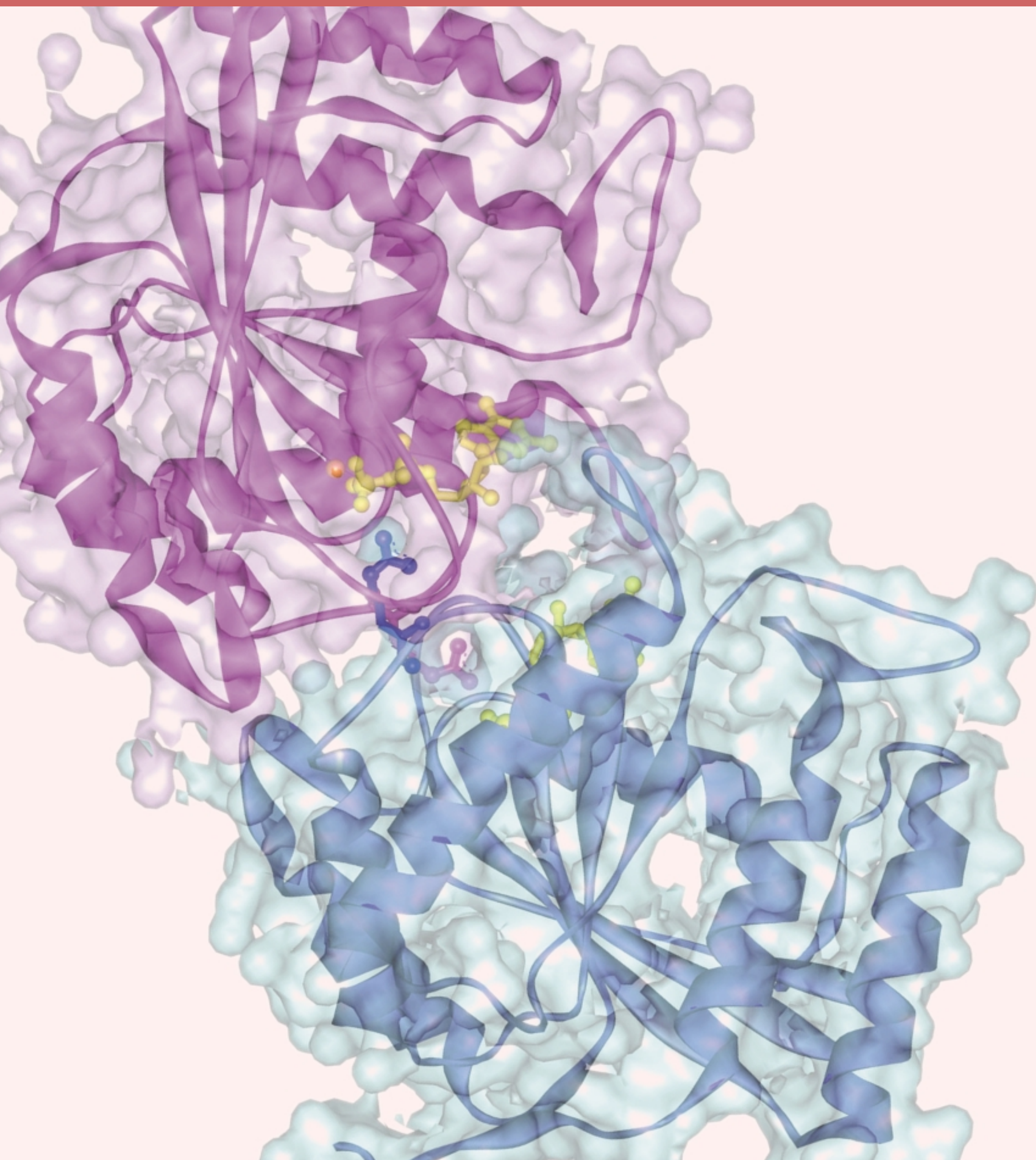

9 Imaging

9-1 Micro X-ray Fluorescence Imaging without Scans

Microscopic imaging that is capable of distinguishing chemical composition is of extreme importance as a scientific tool. X-ray fluorescence (XRF) has been used in routine analysis for the identification and determination of elements contained in specimens in environmental and life sciences as well as in industrial products [1]. The use of synchrotron X-rays as an excitation source is suitable for a wide range of applications because of their non-destructive nature and also because of the absence of charging effects even for insulators and/or organic materials. Recent progresses in synchrotron microbeam technologies have made micro XRF extremely attractive and feasible in many kinds of scientific applications [2]. The imaging, however, usually requires a fairly long measuring time, because the technique uses 2D step scans. This can sometimes be a big problem especially when pixel numbers increase to enhance the quality of the image.

The novel idea presented here is much more rapid XRF imaging. The technique uses a combination of grazing-incidence geometry (0-2 deg) using a rather wide beam (~1 cm) and parallel optics for detecting X-rays by a two-dimensional detector [3,4]. Figure 1 shows a photograph of the present XRF microscope installed at BL-4A. A CCD camera is mounted on the frame with a downward-looking arrangement. The sample has XY stages like a usual optical microscope, and several manual stages for height (i.e, distance to the camera) and tilting. Instead of employing any focusing optics, the natural linear shape of the synchrotron beam is used. The size is 0.2 mm(V) x 12 mm (H). Initially, the technique used total reflection (typically smaller than 1 deg) and was therefore considered as a method to be employed mainly for the imaging of mirror-polished surfaces [3]. However, primary X-rays impinged at approximately 1-2 deg can illuminate the sample, thus creating a contrast corresponding to elements by generating X-ray fluorescence, not only from the surface but also from deeper parts of the specimen. We can accept quite normal specimens, which do not have perfectly flat and smooth surfaces as well. Therefore, the technique is now used for more general imaging in a wide variety of applications.

Figure 2 shows typical examples of XRF imaging [5]. The spatial resolution is only around 20 μm, but, it should be noted that imaging with approximately 1M-pixels can be performed in only 1-2 min, or even less. One can see detailed patterns of the precipitation of metallic crystals, aggregation to the specific part in the tissue, and segregation at the mineral interfaces. Although it is possible to perform the experiments even

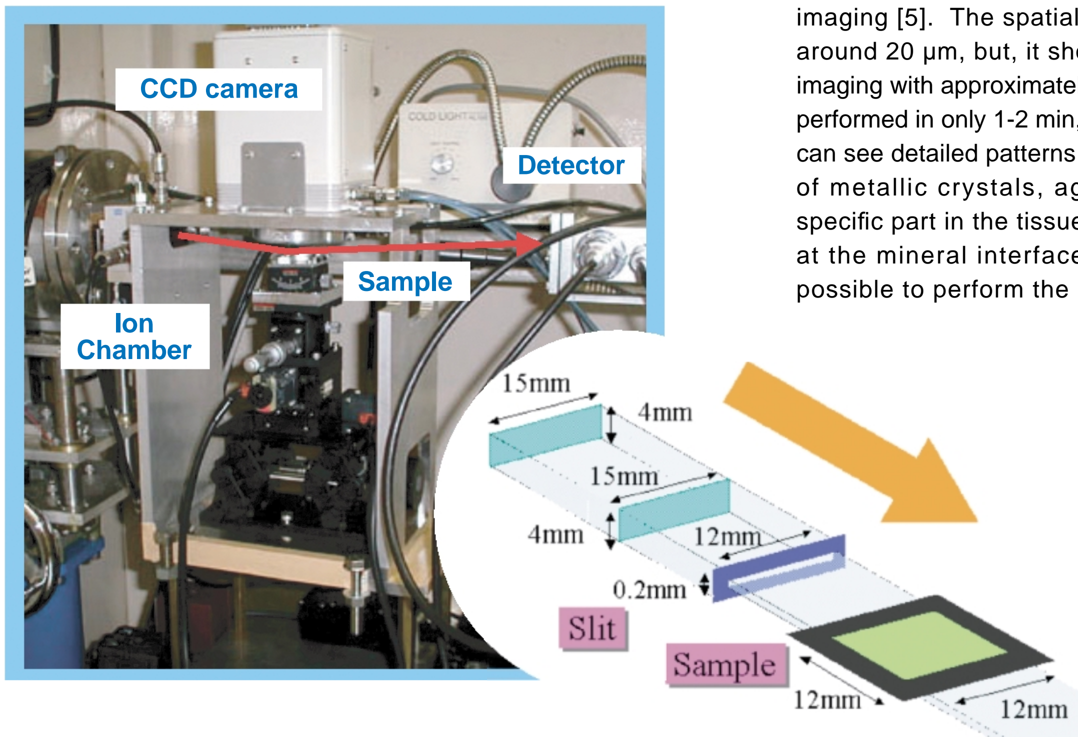

Figure 1
XRF microscope for movie applications. The camera used is a TC215 CCD (Texas Instruments, 1000×1018 pixels, pixel size 12 μm squared) and Hamamatsu C4880 controller (0.25Hz, 14 bit). The resolution is expressed approximately as the product of the distance and the collimation, of which typical values in the present study are 3 mm and 6 mrad, respectively.

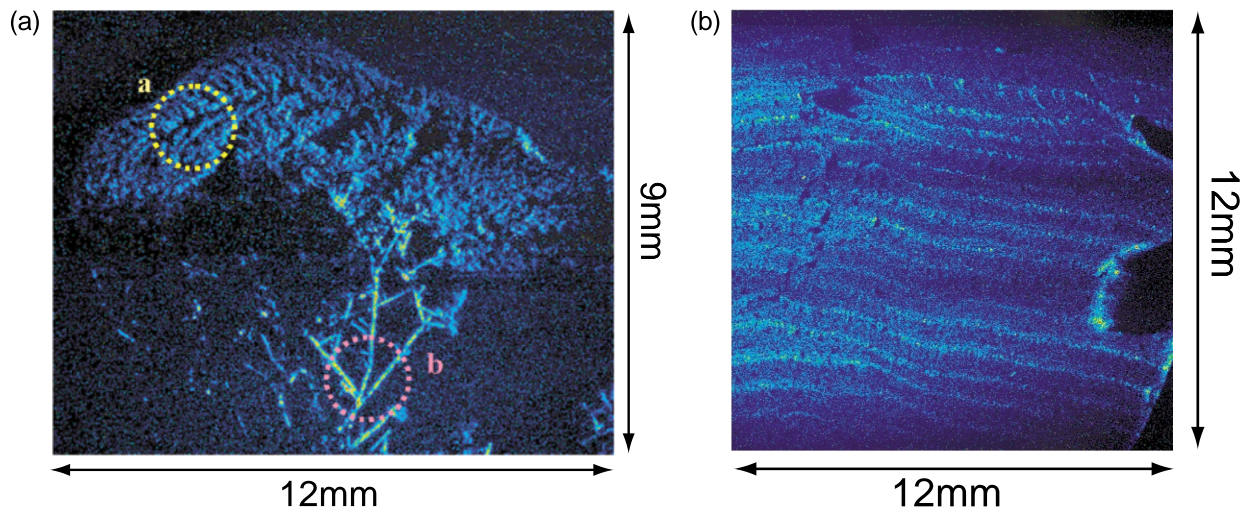

Figure 2
Typical XRF imaging with monochromatic synchrotron beam (7.2 keV). (a) Image of Ag L-X-rays from dendrites grown from a small piece of copper foil, on which a silver nitrate solution is dropped. The pattern changes during the growth: a) final and b) early stages, reflecting the different diffusion velocity. Exposure time 2 min. (b) Rock sample, silicified wood. The stripe pattern is Fe K-X-rays, indicating precipitation of iron in the interfaces. Exposure time 2 min. When the primary beam energy goes below the iron K absorption edge (7.11 keV), Fe K-X-ray fluorescence becomes very dark, and the pattern is not visible.

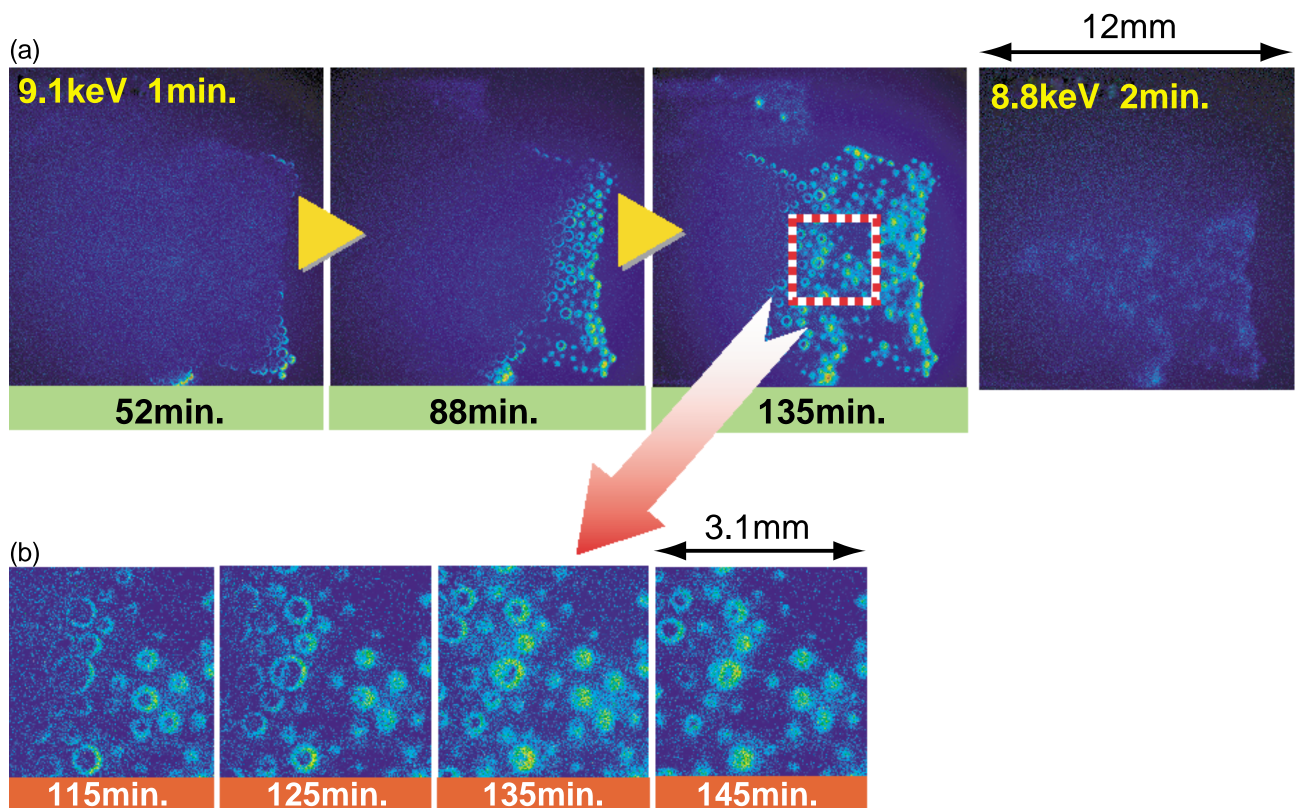

Figure 3
Time dependence of X-ray fluorescence images for the ion exchange resin (Dowex A-1, Dow Chemical Co.) on the wet filter paper with a copper sulfate solution. Primary X-ray energy 9.1 keV. Exposure time 1 min. (a) Images from 52 min to 135 min. (b) Enlarged images from 115 min to 145 min. Scattering X-ray image taken at 8.8 keV (below the copper K edge) is also shown.

with a laboratory X-ray source [3], the use of tunable monochromatic (or quasi-monochromatic) synchrotron X-rays is promising for the selective excitation of the elements contained in the specimen. Another advantage would be the availability of more specific imaging, in addition to information on normal chemical composition, like chemical states, local structure, and atomic location in the periodic structure unit by making use of the X-ray absorption fine structure and X-ray standing waves.

One of the most important advantages of the present non-scanning XRF imaging would be its feasibility in movie applications, because it is possible to repeat the exposure in rather a short time, typically every 40-60 sec in the present case. Figure 3 shows one typical example of a recording movie; successive copper images during ion-exchange reaction [5]. This gave a comprehensive visual description of the exchange starting from the surface of each resin particle, and then the ions being absorbed inside. Since it is possible to obtain separate images for specific elements by choosing primary X-ray energy, one can obtain multi-element movies by quick switching of the monochromator. Further developments are now under way in order to perform more rapid movies in the order of 30-100 msec.

K. Sakurai (NIMS)

References

[1] K. Janssens, F. Adams and A. Rindby, *Microscopic X-Ray Fluorescence Analysis, John Wiley & Sons, London* (2000).
[2] A. Iida, *X-ray Spectrom.* **26** (1997) 359.
[3] K. Sakurai, *Spectrochim. Acta* **B54** (1999) 1497.
[4] K. Sakurai and H.Eba, *Japanese Patent No.3049313* (2000).
[5] K. Sakurai and H.Eba, *Anal. Chem., in press.*

9-2 X-ray Fluorescence Holography for Quantitative Analysis of Local Lattice Distortion

X-ray fluorescence holography (XFH), providing 3D atomic images without any assumption, is a new analytical method for determination of a local environment around a particular element. This technique is not limited to systems with a long-range order, it is also possibly applied to clusters, surface adsorbates and impurities. Applications to doped material (GaAs:Zn) and quasicrystal ($Al_{70.4}Pd_{21}Mn_{8.6}$) has been demonstrated until now. Furthermore, recent advances of the XFH improve the spatial resolution of the atomic images (~0.5 Å FWHM) and visualize light atoms (oxygen). As a next step, we are trying to clarify the local lattice distortions induced by doping and phase transition in a semiconductor, colossal magnetic resistance and superconductor.

"Normal" and "inverse" modes exist in the XFH method. In the normal XFH, depicted in Fig. 4(a),

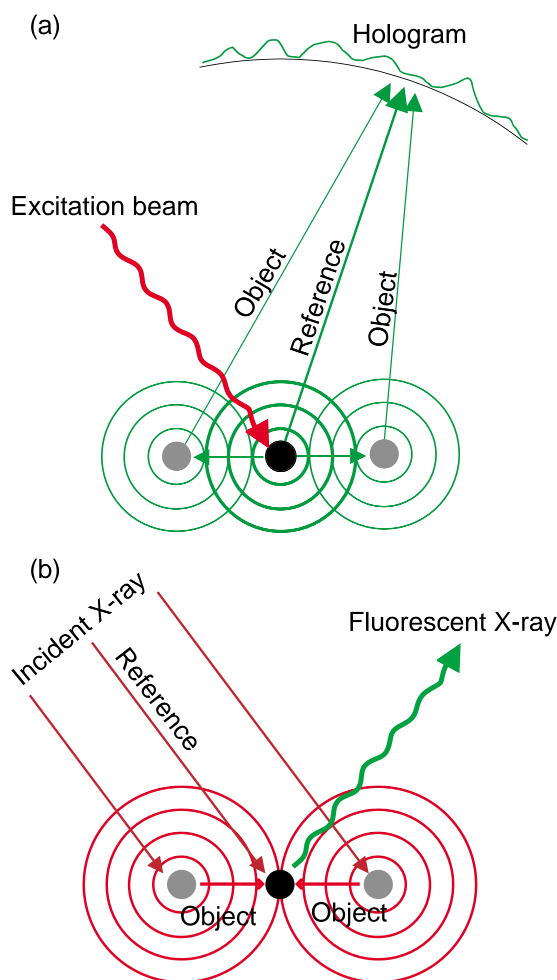

Figure 4
Illustration of XFH principle. (a) Normal and (b) inverse modes.

fluorescence from atoms inside the sample is excited by X-rays or other radiations, such as electron and ion beams. Most of fluorescence from particular emitter atoms which directly enter the detector from the sample, constitutes the holographic reference. Fluorescence scattered by neighboring atoms acts as the holographic object wave, which interferes with the reference beam. By moving the detector on a far-field sphere around the sample, the resulting holographic pattern of the intensity can be recorded. On the other hand, the inverse XFH uses an optical reciprocity theorem of the normal XFH. As shown in Fig. 4(b), the source of radiation and the detector are interchanged. The detector used in the XFH is now replaced by a point source of X-rays, producing a plane wave. The emitter, which formerly served as a source of radiation, becomes a monitor, indicating the electric field strength at its core through the total amount of the fluorescence emitted in all directions. Thus, the incident wave serves as the holographic reference beam, whereas the portion scattered at neighboring atoms, then traveling towards atom, comprises the object beam. Reference and object beams interfere with each other, modulating the electric field at the emitter. By scanning the incident beam in direction, an intensity pattern,

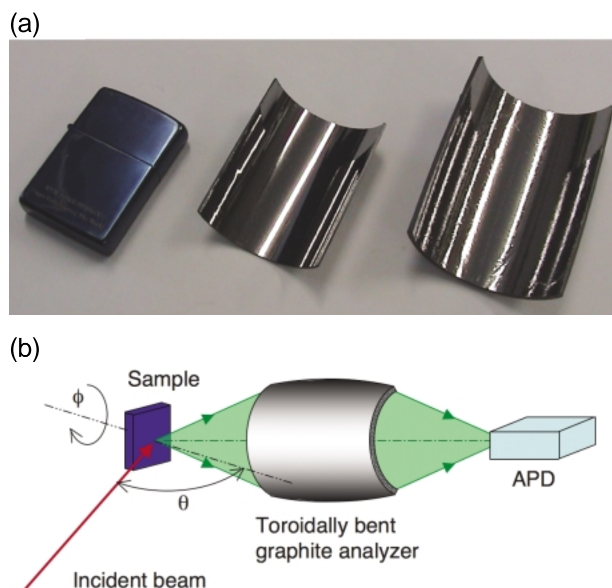

Figure 5
(a) Photograph of bent graphite analyzers. Zippo lighter (left), cylindrically bent graphite (center) and toroidally bent graphite (right).
(b) Experimental setup for fast XFH recording system.

which is equivalent to the hologram in normal mode, is generated. The inverse XFH allows holograms to be recorded at any incident energy above the absorption edge of an emitter.

In order to quantitatively evaluate the local lattice distortion by the XFH, it is essential to record several high-quality holograms at different energies in the inverse mode. Thus, one hologram must be measured within a few hours at most, since the beam time is usually limited to a few days. The holographic oscillation is ~0.1% of its background. This requires that at least one million photons of fluorescence must be colleted at about ten thousand pixels. With a conventional solid-state detector which allows only a low count rate (~ 5000 cps), it takes few months to record a complete hologram. In order to overcome this difficulty, we should adopt a detector with a high count rate as well as with a good energy resolution. We have designed the fast XFH measuring system in combination with a toroidally bent graphite analyzer and an avalanche photodiode (APD) as shown in Fig. 5 [1]. The bent graphite was designed for focusing Cu Kα radiation, and the APD could count in a single-photon counting mode up to ~10^8 cps.

Using this setup, the XFH experiment was demonstrated with a copper single crystal sample at BL-3A. The count rate of Cu Kα attained a few million cps even at the bending magnet beam line. Hologram data of about eighty thousand pixels, which were obtained by scanning the θ and ϕ, were measured within 2.5 hours. Six holograms were obtained with the incident energies ranging from 17.5 to 20.0 keV with 0.5 keV steps. The collected data were processed by normalization with respect to incident intensities, removal of the large

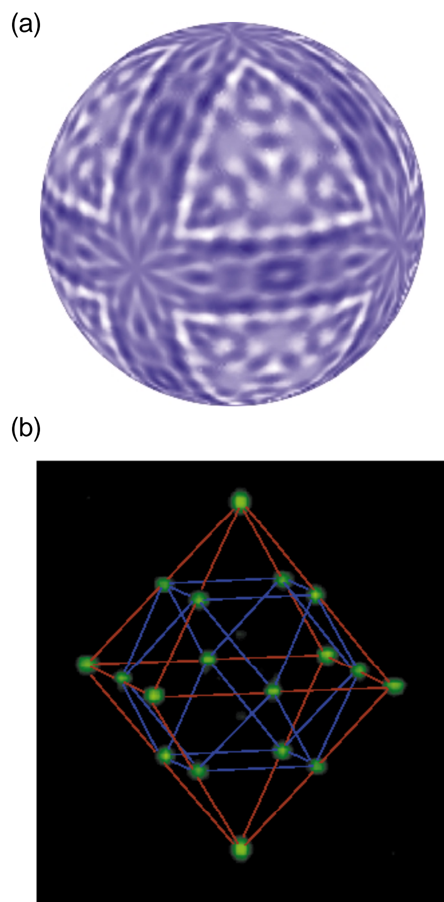

Figure 6
(a) X-ray hologram of Cu single crystal recorded at 18.0 keV.
(b) 3D image of Cu atoms.

background, symmetrization using standing wave lines and low-pass filtering. Figure 6(a) shows a typical hologram pattern of copper recorded at 18.0 keV. The atomic image was reconstructed from six holograms by a modified Fourier transformation algorithm according to Barton. Figure 6(b) shows the 3D atomic image of a copper crystal. First and second neighbor atoms are clearly visible.

One of main reasons why we developed the XFH system for Cu element was analysis of local lattice distortion of copper oxide superconductors [2]. As a preliminary test, a Nd_2CuO_4 single crystal grown at National Institute of Advanced Industrial Science and Technology (AIST), Tsukuba was used as a sample. The X-ray holograms were recorded at 17.0 ~ 19.5 keV (0.5 keV steps). Figure 7 shows the 3D atomic images of Nd_2CuO_4 reconstructed from six holograms. The copper and neodymium atoms neighboring the central copper were clearly visible. To date, most of the XFH experiments have been applied to samples whose crystal structures have high symmetry, such as copper or germanium. The present work proved that the XFH was applicable to a sample with low crystal symmetry. The first nearest oxygen atoms were not recognized in the reconstructed image, which is attributed to several reasons. One is the

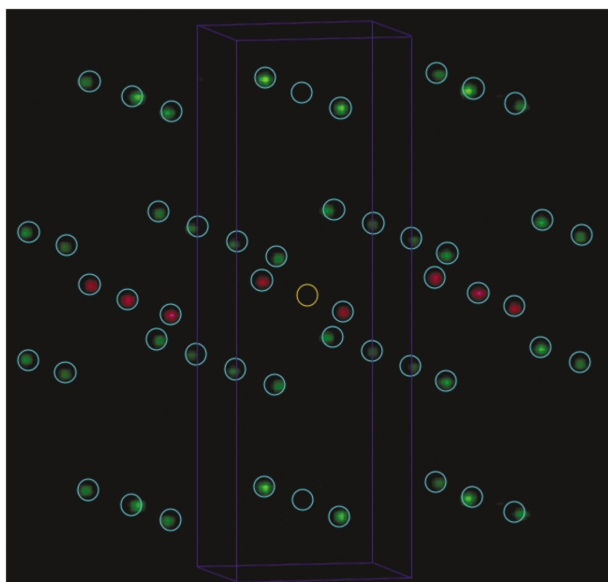

Figure 7
3D image of atomic environment around Cu in a Nd_2CuO_4 single crystal. Red and green atomic images indicate copper and neodymium atoms, respectively.

thermal vibration of the oxygen atoms, much larger than those of the copper and neodymium at room temperature. Since the thermal vibration is suppressed by decreasing the sample temperature, XFH measurement at lower temperature will reveal the oxygen atoms. Another is the scattering cross section of oxygen being lower than that of the other metallic elements. Imaging of oxygen atoms is essential for determination of the local lattice distortion in various functional oxide materials.

K. Hayashi and E. Matsubara (Tohoku Univ.)

References

[1] K. Hayashi, Y. Takahashi, E. Matsubara, S. Kishimoto, T. Mori, M. Tanaka, S. Hayakawa and M. Suzuki, Proceedings of *"The Fourth Pacific Rim International Conference on Advanced Materials and Processing"* (eds. S. Hanada, Z. Zhong, S.W. Nam and R.N. Wright), p. 567-570, The Japan Institute of Metals, Honolulu, 2001.
[2] E. Matsubara, *Ceramics Japan* **37** (2002) 452.